EFFECT OF THE SIMULTANEITY OF EARTHQUAKE COMPONENTS IN STRUCTURES WITH TORSIONAL IRREGULARITY

EFECTO DE LA SIMULTANEIDAD DE LAS COMPONENTES DE SISMO EN ESTRUCTURAS CON IRREGULARIDAD TORSIONAL

Kevin Ortiz [1]* [ID]**, Hugo Scaletti**[2] [ID]

[1]*Departamento de Investigación, Servicio Nacional de Capacitación para la Industria de la Construcción, Lima, Perú*

[2]*Facultad de Ingeniería Civil, Universidad Nacional de Ingeniería, Lima, Perú*

ABSTRACT

The estimation of the maximum design responses according to the current Peruvian technical standard NTE E.030 is carried out considering seismic action as unidirectional. The design spectral acceleration parameters are based on Ground Motion Models which use the geometric mean of the EW and NS earthquake components to define the horizontal component of acceleration, which is always less than the maximum component; hence they are on the unsafe side. Furthermore, even with the correct seismic intensity, the simultaneous action of both components may result in larger demands than those computed by considering only one component at a time. Buildings that would be most affected would be those with torsional irregularity. In this article the most used definitions of horizontal seismic component have been revised, comparing seismic records of events from subduction sources. Then, using both recorded motions and artificial records, simplified models with different degrees of torsional irregularity were analyzed, observing a clear trend in the amplification of the response regarding relative in-plan eccentricity and torsional stiffness. Following the seismic analysis of actual reinforced concrete buildings, it was concluded that the irregularity factor Ip, defined in the NTE E.030, does not compensate the effect of the simultaneity of the components in structures with torsional irregularity. For this reason, this work gives some recommendations to combine the results of the analysis in each orthogonal direction, both for structures with regular configuration and for those categorized as torsionally irregular, and evaluates the future changes in a new version of the NTE E.030 standard.

Keywords: Torsional Irregularity, simultaneous action of earthquake components, in-plan eccentricity

RESUMEN

La estimación de las respuestas máximas de diseño de acuerdo con la norma técnica peruana vigente NTE E.030 se realiza considerando la acción sísmica como unidireccional. Los parámetros de aceleración espectral de diseño se basan en leyes de atenuación que utilizan la media geométrica de los componentes sísmicos EW y NS para definir el componente horizontal de la aceleración, el cual siempre es menor que el componente máximo; por lo tanto, no están del lado de la seguridad. Además, incluso con la intensidad sísmica correcta, la acción simultánea de ambos componentes puede generar demandas mayores que las que se calculan considerando solo un componente a la vez. Los edificios que se verían más afectados serían aquellos con irregularidad torsional. En este artículo se han revisado las definiciones más utilizadas del componente sísmico horizontal, comparando registros sísmicos de eventos provenientes de fuentes de subducción. Luego, utilizando tanto movimientos registrados como registros artificiales, se analizaron modelos simplificados con diferentes grados de irregularidad torsional, observando una clara tendencia en la amplificación de la respuesta con respecto a la excentricidad relativa en el plano y la rigidez torsional. Tras el análisis sísmico de edificios reales de concreto armado, se concluyó que el factor de irregularidad Ip, definido en la NTE E.030, no compensa el efecto de la simultaneidad de los componentes en estructuras con irregularidad torsional. Por esta razón, este trabajo ofrece algunas recomendaciones para combinar los resultados del análisis en cada dirección ortogonal, tanto para estructuras con configuración regular como para aquellas categorizadas como torsionalmente irregulares, y evalúa los posibles cambios en una nueva versión de la norma NTE E.030.

Palabras Clave: Irregularidad torsional, acción simultanea de las componentes de sismo, excentricidad en planta

---

[1] * Corresponding author:
E-mail: kevin.ortiz.st@gmail.com

1. INTRODUCTION

The current E.030 standard of the Peruvian National Building Code [1] states that "For regular structures, seismic analysis may be performed assuming that the total seismic force acts independently in two predominant orthogonal directions." Similarly, "For irregular structures, it must be assumed that the seismic action occurs in the most unfavorable direction." This contrasts with the provisions of various other standards, which specify the simultaneous application of 100% of the seismic force in one direction and a fraction of it in the transverse direction. While it might be assumed that treating the two components separately could be adequate for regular structures [2] , this is not the case. The definition of seismic action in the E.030 standard relies on the estimation of the geometric mean of the maximum forces in two orthogonal directions, since the seismic hazard maps that define the seismic factor Z were developed using ground motion prediction equations by Youngs et al. and Sadigh et al., both of wich characterize horizontal ground motion as the geometric mean of the two horizontal components [1], [3] [4] [5] . Thus, even in the idealized case of perfect regularity, the methodology of the E.030 standard warrants further discussion. The importance of considering both components simultaneously becomes even more significant for structures with torsional irregularity.

In this paper, the effects of the simultaneity of seismic components are analyzed, using earthquake records applied to simple models. The analysis is subsequently extended to include a limited set of existing buildings with varying degrees of irregularity. While the effects of bidirectionality are not as clearly quantified in these buildings as in the simplified models, the results provide technical evidence that may support future updates or refinements to the provisions of the E.030 standard.

This paper is structured as follows: The Background section introduces the context of the study. The Methodology covers the seismic records, a simplified three-degree-of-freedom model, and the analysis of both simplified and real structures with different irregularities. It also includes modal analysis and combination criteria. The paper ends with Conclusions summarizing key findings.

2. BACKGROUND

The predictive equations for ground motion in terms of peak horizontal acceleration and velocity, and for response spectral ordinates, have used various definitions for the horizontal component of motion. These definitions are based on different treatments of the two horizontal components in each analyzed seismic record. This distinction becomes particularly important when structural analysis considers bidirectional seismic loading [6].

In seismic design, the goal is to determine the maximum response of a structure under external loads, allowing the design of a system that can resist these forces. The acceleration from a seismic zoning study is derived from attenuation laws that are combined through a decision tree and typically define the horizontal component as the geometric mean of the orthogonal horizontal components as recorded. This geometric mean is always smaller in magnitude than the maximum horizontal component recorded in any one direction; thus, the maximum structural response is underestimated.

On the other hand, the E.030 standard allows the maximum response to be obtained from separate analysis in each of two orthogonal directions, without accounting for the simultaneous effect of the components. In structures with regular floor plans, the simultaneity of components is not particularly significant [7]; however, this may not be the case for buildings with irregular floor plans. The variable here is the relationship between calculating this response by considering component simultaneity versus independent action in a single direction [7] [8].

Plan eccentricity in a building, due to the configuration of the lateral force-resisting system, results in a torsional moment that amplifies responses in the perimeter elements. This amplification increases with the degree of torsional irregularity and the magnitude of the component in the direction orthogonal to the eccentricity. Therefore, there is considerable uncertainty in calculating the maximum response of a structure with torsional irregularity under bidirectional seismic loading.

Seismic codes worldwide handle the issue of component simultaneity by performing unidirectional analyses and combining effects in each direction using the square root of the sum of squares, adding a fraction of the effect in the other orthogonal direction, or amplifying the maximum effect in one direction by a defined factor, among other methods. Various authors have compared the different recommendations for combining the response components in orthogonal directions.

For instance, Fernández et al. [9], in their study "Considering the Bi-Directional Effects and the Seismic Angle Variations in Building Design,"

performed nonlinear analyses on multi-story buildings subjected to seismic inputs applied at varying angles, including bidirectional ground motions. Their results show that common combination rules may underestimate demands in certain directions, and they conclude that there is no consistent correlation between the structural configuration and the response obtained under bidirectional seismic action.

Hisada et al. [7] conducted numerical simulations using simplified SDOF and MDOF models to evaluate orthogonal effects, focusing on how bidirectional ground motions influence internal forces and response patterns. They emphasized the importance of considering orthogonal components in seismic design, as well as the absolute values of the input motions and the design methods used for structural elements. Moscoso [8] analyzed the impact of bidirectionality and seismic incidence angle on reinforced concrete structures through linear and nonlinear time-history analyses, using multiple Peruvian ground motions and deriving amplification factors based on the comparison with spectral modal analysis.

In any case, it is necessary to review the E.030 standard regarding component simultaneity and propose simple rules to allow for safe estimates of possible effects.

3. METHODOLOGY

In this paper, simplified three-degree-of-freedom models and existing building models with different levels of irregularity were studied using linear analysis with both real and artificial seismic records.

3.1. Seismic records

The seismic events used in the analysis occurred in Perú and Chile, with magnitudes ranging from 7.9 to 9.9 Mw, hypocentral depths between 24 and 40 km, and epicentral distances from 125 to 415 km. The fault mechanisms of these events were of the interface subduction type. The ASCE 7 [10] defines near-field records as those recorded within 15 km of the source (for magnitudes greater than 7 Mw). In this study, the records used would be classified as far-field and were corrected by baseline and bandwidth filter. TABLE I contains the information about the records used in this work. Additional information is presented in reference [15].

3.2. Characterization of the Three-Degree-of-Freedom Simplified Model

Numerical models of real buildings are complex and have many degrees of freedom, which would require considerable effort to perform a parametric analysis relating the degree of torsional irregularity to the effect of simultaneous seismic components. Additionally, each model presents specific stiffness distributions and types of irregularities, making generalization of results difficult. For this reason, as the first stage of the study, single-story models with regular geometric floor plans are proposed. The floor plan model has two main axes, X and Y. The floor plan eccentricity of the model is represented by a lateral stiffness configuration, which shifts the center of rigidity (CR) a distance e_x from the center of mass (CM). This model enables the evaluation of the effects of the simultaneous application of seismic components in relation to the floor plan eccentricity, which defines the degree of torsional irregularity G_{ti}.

The simplified model has three degrees of freedom: two translational (in the X and Y directions) and one rotational (around the Z-axis). The eccentricity of the floor plan model is defined as the distance e_x. A graphical representation of the model is shown in Fig. 1.

The proposed model can be geometrically characterized by a dimension in plan called B, and a side ratio α_p. In terms of its stiffness properties, these will be parameterized using a lateral vibration period, T_x, which correspond to the model vibration in the X direction. Additionally, a rigidity ratio, α_k, is

TABLE I
Summary table of Record Classification Based on Soil Profile

Seismic Event	Magnitude (Mw)	Record	Vs_{30}	Classification NTE E.030
Maule	8.8	Angol	334	S2
		Maipu	450	S2
Atico	8.4	CVV	764	S1
Pisco	7.9	UNICA	250	S2
Huacho	8.1	PRQ	857	S1

Note: The values of Vs_{30} were calculated according to the E.030 standard [1], using the information from shear wave velocity profiles of the corresponding accelerometric stations.
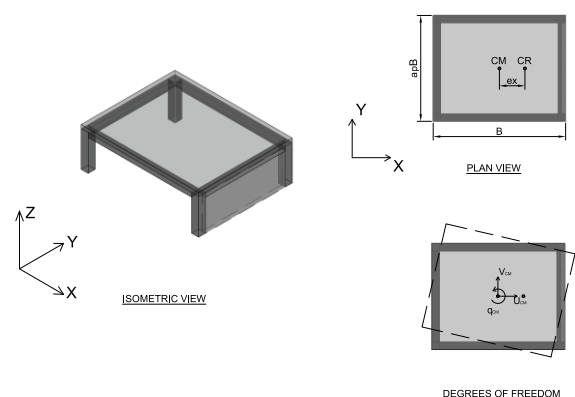[11],[12],[13],[14]

Fig. 1. Simplified model with three degrees of freedom.

introduced, representing the proportion between the lateral periods in the Y and X directions.

The model mass distribution per unit area, ρ_a, is also considered, and the mass of the model is calculated with equation (1).

The lateral stiffness in X, k_x, is calculated using equation (2).

The torsional moment of inertia around the Z axis is given by equation (3).

The torsional stiffness is calculated with equation (4). This property depends on the lateral stiffness, k_x, the dimension B, and a torsional stiffness factor f. This factor is the product of a shape factor, f_s, which is calculated with equation (5), and a distribution factor f_d, which is based on the distribution of lateral stiffness in both directions in plan. Extreme values of f = 0.10 and f =0.5 were considered, which include with wide margins the expected values in real structures.
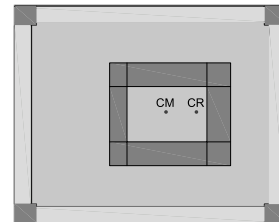
$$k_r = f k_x B^2 \dots\dots\dots\dots\dots\dots(4)$$

$$f_s = \frac{\alpha_p{}^2 + \alpha_k}{2} \dots\dots\dots\dots\dots\dots(5)$$

In Fig. 2(a), the stiffness is assumed to be localized at the boundary, representing a theoretical case. In this scenario, the distribution factor is 0.5, the maximum expected value for this factor. Fig. 2(b) illustrates a case where lateral stiffness is located at internal axes, and for this case the value of f_d is lower than 0.5.
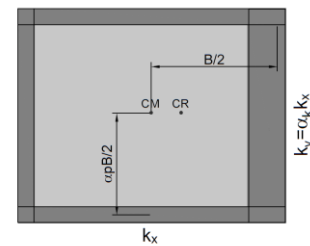
LATERAL STIFFNESS LOCALIZED AT THE BOUNDARY

(a)

LATERAL STIFFNES LOCALIZED AT INTERNAL AXES

(b)

Fig. 2. Stiffness distribution models

The structural analysis of the simplified models was performed as pseudo-three-dimensional. The translation of the center of mass of the model in the X direction was defined as degree of freedom DOF 1, its translation in the Y direction as DOF 2, and the rotation of the diaphragm about the Z axis as DOF 3.

The corresponding stiffness and mass matrices are calculated according to equations (6) and (7).

The torsional irregularity degree of the model, G_{ti}, is defined as the ratio between the maximum displacement Δ_{max} and the displacement of the center of mass Δ_{CM}, subjected to a static load P in the direction orthogonal to the eccentricity. Fig. 3 shows a diagram of the static analysis performed on the model to define the torsional irregularity degree.

Considering the behavior of the rigid diaphragm, the torsional irregularity degree was calculated by solving the equilibrium equations. Equation (8) illustrates the relationship between the degree of torsional irregularity and the model properties. From this equation, it can be observed that the torsional irregularity degree depends only on the relative eccentricity, the rigidity ratio, and the torsional stiffness factor.

$$G_{ti} = 1 + \frac{\alpha_k \left(\frac{e_x}{B}\right)}{2f} \dots\dots\dots\dots\dots\dots(8)$$

$$u = \sum_{i=1}^{3} a_i \phi_i \dots\dots\dots\dots (10)$$

3.3. Time history analysis of Three-Degree-of-Freedom Simplified Model

The time-history linear analysis was performed as a superposition of the responses of each vibration mode for each time step. The dynamic equation of motion with bidirectional ground acceleration is presented in equation (9).

Where:

- C: Damping Matrix.
- u: Displacement vector of the center of mass
- $\dot{u}$: Velocity vector of the center of mass
- $\ddot{u}$: Acceleration vector of the center of mass
- $\mathbf{1}_x$: First column of the $3x3$ identity matrix.
- $\mathbf{1}_y$: Second column of the $3x3$ identity matrix.
- $\ddot{u}_{gx}$: Ground acceleration record in the X direction.
- $\ddot{u}_{gy}$: Ground acceleration record in the Y direction.

By solving equation (9) using modal superposition, the displacement vector can be expressed

Where:

- a_i: Modal coordinate of the vibration mode i.
- $\boldsymbol{\phi}_i$: Shape vector of the vibration mode i.

By substituting equation (10) into equation (9) and multiplying both sides by $\boldsymbol{\phi}_i^T$, the decoupled

$$\boldsymbol{\phi_1} = \begin{bmatrix} 1 \\ 0 \\ 0 \end{bmatrix} \dots\dots\dots\dots\dots\dots (12)$$

$$\boldsymbol{\phi_{2,3}} = \begin{bmatrix} 0 \\ 1 \\ s \end{bmatrix} \dots\dots\dots\dots\dots\dots (13)$$

vibration equation for each vibration mode i results in the following expression.

Where:

- ω_{ni}: Circular natural frequency of vibration

$$s = \frac{\left(\frac{\omega_n}{\omega_y}\right)^2 - 1}{e_x} \dots\dots\dots\dots\dots\dots (14)$$

  mode i.
- ζ_i: Critical damping fraction of vibration mode i which will be considered equal to 5% for all modes.
- $\dot{a}_i$: Time derivative of the modal coordinate of the vibration mode i.
- $\ddot{a}_i$: Time derivative of order 2 of the modal coordinate of the vibration mode i.
- Γ_x: Participation factor in X direction.

$$\boldsymbol{u}(t) = d_1(t)\boldsymbol{\phi_1} + \left(\frac{m}{m+s_2^2 J}\right) d_2(t)\boldsymbol{\phi_2} +$$
$$\left(\frac{m}{m+s_3^2 J}\right) d_3(t)\boldsymbol{\phi_3} \dots\dots\dots\dots\dots\dots (15)$$

- Γ_y: Participation factor in Y direction.

The mode shapes of the simplified model correspond to a purely translational mode in the X direction and two modes that are combination of

$$\ddot{d}_{2,3} + 2\zeta_{2,3}\omega_{n2,3}\dot{d}_{2,3} + \omega_{n2,3}{}^2 d_{2,3} = -\ddot{u}_{gy} \dots\dots (16)$$
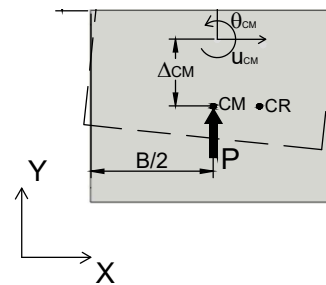

Fig. 3. Static analysis of simplified model

translation along the Y axis and rotation around the Z axis and they are defined as follows:

s is determined solving the eigenvalue and eigenvector problem, and it depends on the plan eccentricity e_x and the ratio between the circular frequencies ω_n and ω_y as follows:

ω_n is obtained solving the characteristic polynomial. Once s is calculated, the participation factors are determined for each mode.
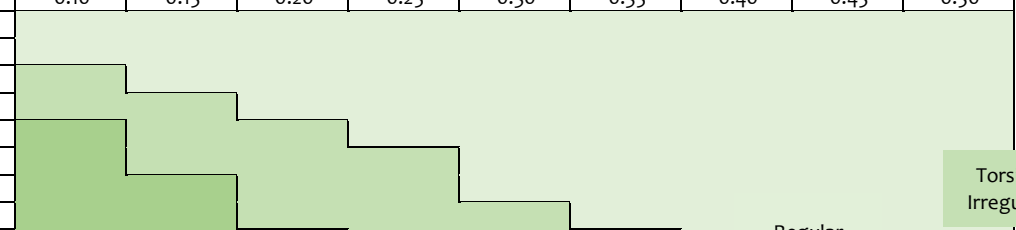
The response at each time t is obtained by superimposing the three modes, as shown in equation (15).

Here, $d_i(t)$ represents the solution to the second-order differential equation for the general problem of a system with one degree of freedom per vibration mode. The ground acceleration in the X direction is applied to vibration mode 1, while the ground acceleration in the Y direction is applied to vibration modes 2 and 3.

3.4. Structural Analysis of the Three-Degree-of-Freedom Simplified Model

In this section, the simplified models of a square plant and of rectangular plant with a 1:2 aspect ratio are analyzed to examine the influence of calculating the maximum responses in the analysis considering the simultaneity of components. Models with equal lateral stiffness in both directions were considered.

TABLE II
Classification of simplified models with a square plan and equal lateral stiffness in each direction

ex/B	f								
	0.10	0.15	0.20	0.25	0.30	0.35	0.40	0.45	0.50
0.025									
0.05									
0.075									
0.1									
0.125									
0.15									
0.175									
0.2								Regular	Torsional Irregularity
0.225									
0.25									

According to the NTE E-030 [1], the limit values that determine the degree of irregularity of a building are 1.3 and 1.5. For a simplified model with $\alpha_k = 1$ and $\alpha_p = 1$, i.e., $f_f = 1$, each model can be classified according to its relative eccentricity e_x/B and its torsional rigidity factor $f = f_d$ as per equation (8).

TABLE II shows the classification of simplified models with a square plan and equal lateral stiffness in each direction. The colors represent the degree of
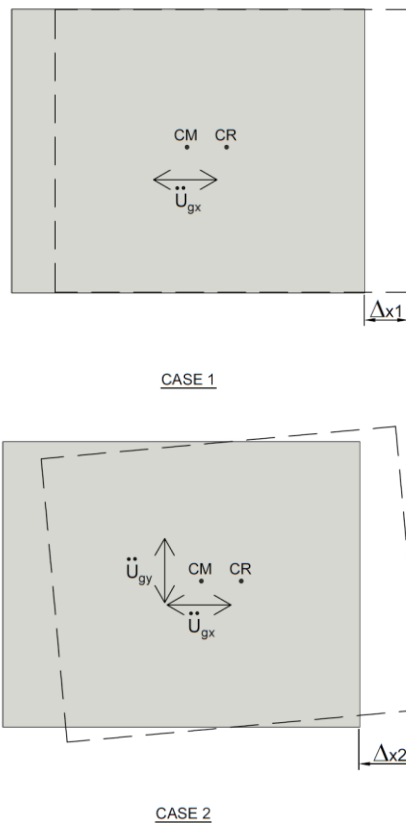

CASE 1

CASE 2

Fig. 4. Diagram of comparative analysis of the simultaneity of components

irregularity of each simplified model, with torsional rigidity factor f and relative eccentricity e_x/B.

To evaluate the maximum effects that the structures with irregularity degrees equivalent to the simplified models could have, acceleration records were used as they were originally recorded, and these are described in TABLE I. Fig. 4 presents the load cases to be compared. The maximum ratio between
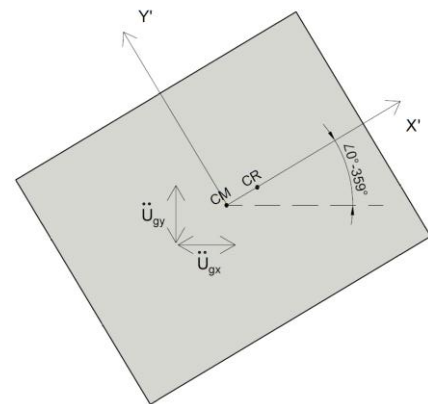
Fig. 5. Rotation of the simplified model

the displacements of case 2 and case 1 $\left(\Delta_{x2}/\Delta_{x1}\right)$ was calculated for each model defined in TABLE II. To eliminate the uncertainty of orientation, the model was rotated from 0° to 359° as shown in Fig. 5.

The values of $\left(\Delta_{x2}/\Delta_{x1}\right)$ were calculated as the maximum for the range of lateral periods from $0.1\ s$ to $1\ s$, rotation range from 0° to 359°, and the real acceleration records considered in this work. These values are shown in TABLE III, where each model is represented by its relative eccentricity e_x/B and its torsional rigidity factor f, displaying the range of amplification values $\left(\Delta_{x2}/\Delta_{x1}\right)$ that each model could have.

For the records studied in this work, the analyzed simplified models show maximum amplifications of 3.02 for models classified as regular according to the NTE E.030 criteria, and 3.66 for models classified as

structures with torsional irregularity. In models classified as structures with extreme torsional irregularity, amplifications of up to 14.26 were calculated for the case of lateral stiffness concentrated near the center of mass.

In general, higher amplification values are observed. For a simplified rectangular plan model, a side ratio of $\alpha_p = 2$ was considered, as it is a common proportion in buildings. For the calculation of the torsional irregularity degree G_{ti}, the maximum displacement would occur in the X direction. Equation (8) would be rewritten as:

Let K be the lateral stiffness of the floor, which is equal in both the X and Y directions. Since the plan eccentricity is in the X direction, the shear walls oriented in this direction have the same lateral stiffness ($0.5K$) and are equidistant from the center of mass (CM). The factor β defines the proportion of stiffness that the shear wall with the smaller section oriented in the Y direction possesses. The plan has a side length of $B = 10m$ in both directions, and the mass is considered concentrated at the CM. Using equation (1) and an area density of $1000\ kg/m^2$ a mass of $100\ ton$ per level was calculated. The

TABLE III

Amplification of the simplified models with a square plan. The table also shows the amplification ranges obtained from the analysis for each

TABLE IV

Classification of simplified models with a rectangular plan and equal lateral stiffness in each direction. The table also shows the amplification ranges obtained from the analysis for each rotation angle of the model

ex/B	f							
	0.20	0.35	0.50	0.65	0.80	0.95	1.10	1.25
0.025	<1.07,1.49>	<1.14,1.82>	<1.08,1.52>	<1.05,1.26>	<1.02,1.16>	<1.02,1.15>	<1.02,1.11>	<1.01,1.09>
0.05	<1.15,1.97>	<1.27,2.53>	<1.17,1.99>	<1.10,1.51>	<1.05,1.34>	<1.04,1.31>	<1.04,1.22>	<1.03,1.18>
0.075	<1.23,2.38>	<1.34,3.07>	<1.30,2.39>	<1.15,1.75>	<1.09,1.51>	<1.06,1.46>	<1.06,1.33>	<1.05,1.27>
0.1	<1.32,2.84>	<1.51,3.59>	<1.44,2.75>	<1.20,2.03>	<1.13,1.69>	<1.09,1.61>	<1.08,1.44>	<1.06,1.36>
0.125	<1.39,3.48>	<1.69,4.00>	<1.48,3.11>	<1.25,2.34>	<1.18,1.88>	<1.12,1.76>	<1.10,1.55>	<1.08,1.44>
0.15	<1.44,4.53>	<1.61,4.11>	<1.53,3.44>	<1.30,2.64>	<1.20,2.07>	<1.16,1.90>	<1.13,1.65>	<1.10,1.52>
0.175	<1.50,6.36>	<1.62,4.08>	<1.54,3.53>	<1.38,2.97>	<1.26,2.25>	<1.18,2.03>	<1.16,1.75>	<1.11,1.59>
0.2	<1.54,8.33>	<1.73,4.18>	<1.61,3.34>	<1.41,3.14>	<1.32,2.42>	<1.19,2.18>	<1.18,1.85>	<1.13,1.65>
0.225	<1.60,8.71>	<1.73,4.28>	<1.63,3.48>	<1.41,3.10>	<1.39,2.57>	<1.23,2.33>	<1.20,1.94>	<1.16,1.72>
0.25	<1.64,9.42>	<1.78,4.54>	<1.66,3.56>	<1.41,3.22>	<1.44,2.68>	<1.27,2.47>	<1.23,2.03>	<1.18,1.77>

For the simplified models with $\alpha_k = 1$ and $\alpha_p = 2$ the value of f_f is 2.5; each model can be classified according to its relative eccentricity and its torsional rigidity factor using equation (17). Since f_d can take a maximum value of 0.5, f can reach a value of up to 1.25. The classification of each model is shown in TABLE IV.

For models with $\alpha_p > 2$, it can be assumed that the amplification ranges will be of the same order of magnitude. Therefore, it is observed that the effect of considering the simultaneity of seismic components is important even for structures classified as regular, and the procedures established in the NTE E.030[1] must be reconsidered.

3.5. Structural Analysis of a Simplified Multi-Level Model

To evaluate the influence of the number of levels, nine square plan models were proposed with equal lateral stiffness in both the X and Y directions. All models have a plan eccentricity in the X direction of 0.25 for all levels. In the structural analysis, deformations in the Z axis were not considered, the slabs were treated as membrane-type elements, and the shear walls were modeled as frame type elements. The configuration of each floor is shown in Fig. 6.
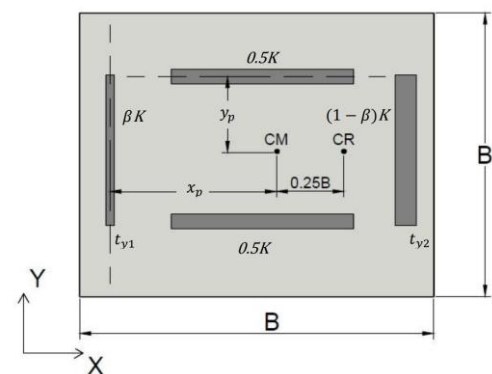

Fig. 6. Plan configuration of simplified multi-level models.

torsional moment of inertia was calculated using equation (3), resulting in a value of J equal to $1666.67\ ton.m^2$ per level.

In the analysis of the lateral stiffness of the shear walls, only the contribution of shear stiffness was considered. The contribution of each wall to the lateral stiffness is defined by the ratio of their thicknesses, which is equivalent to the factor β. The four walls have a length of $4m$ and a height of $3m$ per level. The walls oriented in the X direction have a thickness of $30cm$, and the thicknesses t_{y1} and t_{y2} of the walls oriented in the Y direction must sum to $60cm$ and be related to the factor β. TABLE V presents the values that define the plan configuration of the simplified models for each value of f.

TABLE V
Values that define the plan configuration for different torsional rigidity factors

f	$x_p(m)$	$y_p(m)$	β	$t_{y1}(cm)$	$t_{y2}(cm)$
0.1	3.00	1.00	0.08	5	55
0.3	4.90	2.45	0.24	15	45
0.5	5.00	5.00	0.25	15	45

It was assumed that each model has a fundamental period $T_X = 0.08N$, where N is the number of levels in the model, and T_X is expressed in seconds. The modulus of elasticity of the material of the walls was adjusted so that the lateral vibration modes of the models have periods of $0.4\ s$, $0.8\ s$ and $1.6\ s$ for the 5, 10, and 20-level models, respectively. Fig. (7) shows the lateral vibration mode of the simplified 10-level model with a factor $f = 0.3$ and a vibration period of $0.795\ s$.
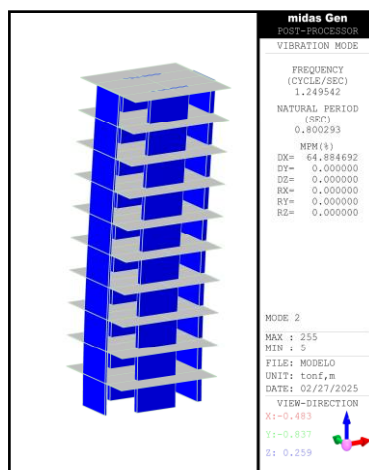

Fig. 7. Lateral vibration mode of the simplified model with a torsional irregularity factor f=0.3 and 10 levels.

Analogous to the analysis conducted in the previous sections, linear time-history analyses were performed using the Angol and UNICA records, with rotations every 30° from 0° to 90°. The maximum drifts in the X direction were calculated. TABLE VI presents the summary of the amplification ranges for the nine simplified models.

By comparing TABLE II and TABLE VI it is concluded that the amplifications are smaller for

TABLE VI
Values that define the plan configuration for different torsional rigidity factors

N	$T_x(s)$	f		
		0.1	0.3	0.5
5	0.4	<1.03;2.85>	<1.06;1.56>	<1.08;1.26>
10	0.8	<1.07;2.58>	<1.01;1.7>	<1.00;1.28>
20	1.6	<1.03;3.37>	<1.04;1.83>	<1.01;1.25>

multi-level models. In the case of $f = 0.1$, the amplifications are much lower, decreasing from 14.26 to 2.85. This significant difference requires further study. Amplifications remain significant for torsional irregularity factors of 0.3 and 0.5.

3.6. Analysis of structures with different degrees of irregularity

The cases analyzed in this section correspond to existing building structures evaluated in a 2020 report by SENCICO [15]. The study evaluated how considering the simultaneity of seismic components affects the calculation of maximum responses used in seismic design. Additionally, the procedures outlined in NTE E.030[1] were reviewed.

The buildings were selected with varying degrees of torsional irregularity, ranging from minor to major

TABLE VII
Dynamic Properties and Degrees of Torsional Irregularity of Buildings Considered in the Study

Model	N	Fundamental Period T(s)	G_{tiX}	G_{tiY}	G_{ti}
1	5	0.106	1.006	1.052	1.052
2	12	1.387	1.057	1.062	1.062
3	21	1.692	1.022	1.097	1.097
4	10	0.997	1.124	1.073	1.124
5	18	2.556	1.075	1.248	1.248
6	7	0.485	1.126	1.269	1.269
7	7	0.575	1.276	1.084	1.276
8	9	1.109	1.305	1.256	1.305
9	17	2.030	1.353	1.155	1.353
10	21	2.239	1.404	1.358	1.404
11	5	0.376	1.243	1.427	1.427
12	21	3.018	1.463	1.349	1.463
13	16	1.699	1.470	1.449	1.470
14	8	0.604	1.304	1.500	1.500
15	11	1.160	1.552	1.285	1.552
16	12	1.820	1.573	1.146	1.573
17	8	1.428	1.642	1.206	1.642
18	15	1.732	1.482	1.866	1.866

as shown in the TABLE VII. Basements were modeled as additional floors, and the weight of the structure was calculated as the sum of 100% of the dead load and a percentage of live load, depending on the

seismic category of the structure. Office and residential building models were classified as Category C buildings (ordinary structures) according to NTE E.030 [1], where 25% of the live load is considered for the estimation of the structural weight. The school building model was classified as a Category A building (essential structure) according to NTE E.030, where 50% of the live load is considered for the estimation of the structural weight. Dead and live load patterns vary for each building but are consistent with NTE E.020 [16].

For each building model, the degree of torsional irregularity G_{ti} of each diaphragm was calculated using dynamic analysis with spectral modal superposition, considering 5% accidental eccentricity. The representative value of G_{ti} for each building was taken as the maximum value calculated for any diaphragm. The degrees of torsional irregularity were also calculated considering the maximum responses in the X and Y directions.

The models presented were analyzed using the records from the Angol, UNICA and Atico stations described in 3.1. To evaluate the effect of the simultaneity of components, three loading cases were analyzed as follows:

- Case 1: Application of the record components simultaneously, where the EW component is applied in the X direction and the NS component in the Y direction.
- Case 2: Application of the EW component of the record in the X direction.
- Case 3: Application of the NS component of the record in the Y direction.

To assess the effects of the building orientation, the X and Y axes were rotated by $30°$, $60°$ and $90°$, and the accelerations of the records were projected onto the rotated axes.

For each model, a comparison of the maximum inter-story drifts was performed using time-history analysis with the following procedure:
- Identify the level with maximum inter-story drift from Case 1, considering the maximum drift calculated for records whit no rotation and those rotated by $30°$, $60°$ and $90°$.
- Once the level with maximum drift for each record is identified, apply Case 2 and Case 3.
- Calculate the simultaneity ratios for each record.

The relationship between the responses considering the simultaneity of components is represented by the simultaneity ratios A_X and A_Y, defined as follows:

$$A_X = \frac{F_{X,Sim}}{F_{X,Uni}} \dots\dots\dots\dots\dots\dots(17)$$

$$A_Y = \frac{F_{Y,Sim}}{F_{Y,Uni}} \dots\dots\dots\dots\dots\dots(18)$$

Where:

- $F_{X,Uni}$: Maximum elastic response in the X direction produced by unidirectional seismic action.
- $F_{Y,Uni}$: Maximum elastic response in the Y direction produced by unidirectional seismic action.
- $F_{X,Sim}$: Maximum elastic response in the X direction produced by bidirectional seismic action.
- $F_{X,Sim}$: Maximum elastic response in the Y direction produced by bidirectional seismic action.

The results are presented in Fig. 8, Fig. 9 and Fig. 10. L_1 marks the threshold between structures classified as regular and irregular, according to NTE E.030. L_2 represents the lower limit of extreme irregularity, also defined by NTE E.030 [1].

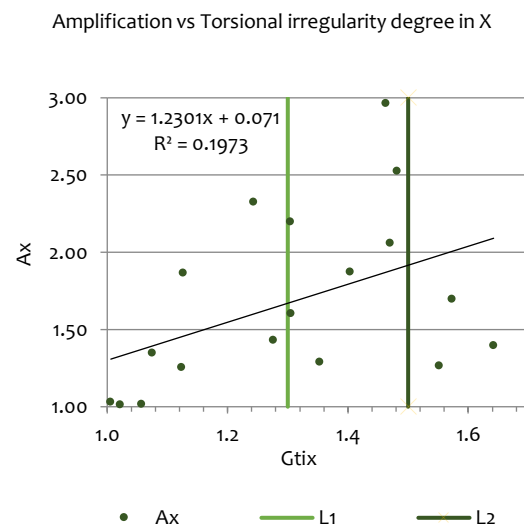Amplification vs Torsional irregularity degree in X

Fig. 8. Simultaneity amplifications for each evaluated model calculated using the responses in the X direction.

A significant dispersion is observed in Fig. 8 and Fig. 9, in contrast to Fig. 10, where the maximum amplification in both directions is plotted against the torsional irregularity degree, as specified in NTE E.030 [1].
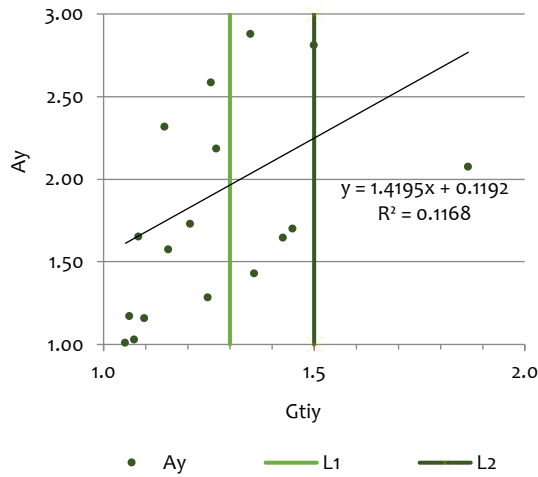
Fig. 9. Simultaneity amplifications for each evaluated model calculated using the responses in the Y direction.
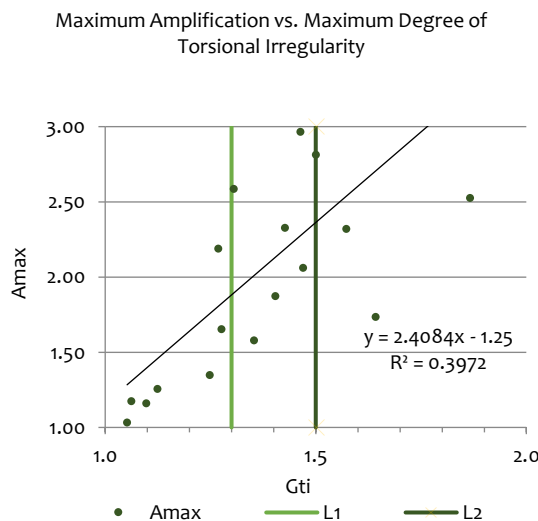

Fig. 10. Maximum Simultaneity Amplifications for Each Evaluated Model Compared to the Maximum Degree of Torsional Irregularity.

3.7. Spectral Modal Analysis of the Studied Models

The analysis considered the elastic design spectrum from the NTE E.030[1], with the following parameters: $Z = 0.45, U = 1, S = 1, T_p = 0.4\ s$ and $T_l = 2.5\ s$, and inter-story drifts were compared with unidirectional analyses as specified in the standard. Additionally, drifts were calculated using sum type combination criterion, which involve applying 100% of the action in one direction and 30%, 85%, or 100% in the orthogonal direction.

The maximum spectral amplification was calculated using the following equations:

$$A_{SX} - \alpha\% = \frac{\gamma_{X,X} + \alpha\%\gamma_{Y,X}}{\gamma_{X,X}} \dots\dots\dots (19)$$

$$A_{SY} - \alpha\% = \frac{\gamma_{Y,Y} + \alpha\%\gamma_{X,Y}}{\gamma_{Y,Y}} \dots\dots\dots (20)$$

$$A_{SMAX} - \alpha\% = max(A_{SX} - \alpha\%, A_{SY} - \alpha\%) \ \dots(21)$$

Where:

- $\gamma_{X,X}$: Maximum inter-story drift in the X direction calculated from the unidirectional spectral modal analysis in X.
- $\gamma_{Y,Y}$: Maximum inter-story drift in the Y direction calculated from the unidirectional spectral modal analysis in Y.
- $\gamma_{X,Y}$: Maximum inter-story drift in the X direction calculated from the unidirectional spectral modal analysis in Y.
- $\gamma_{X,Y}$: Maximum inter-story drift in the X direction calculated from the unidirectional spectral modal analysis in Y.
- $\alpha\%$: Combination factor.
- $A_{SX} - \alpha\%$: Spectral amplification calculated as the ratio of maximum drift in the X direction for the sum combination of $\alpha\%$.
- $A_{SY} - \alpha\%$: Spectral amplification calculated as the ratio of maximum drift in the Y direction for the sum combination of $\alpha\%$.
- $A_{SMAX} - \alpha\%$: Maximum spectral amplification for the sum combination of $\alpha\%$.

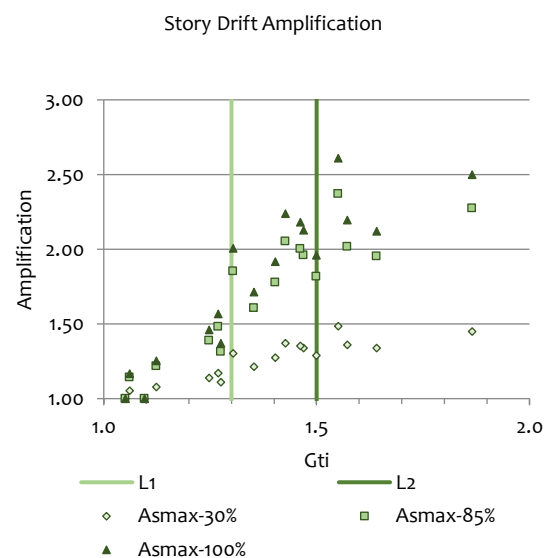By conducting the analyses on the eighteen studied models, the results are presented in Fig. 11.

Fig. 11. Comparison of maximum amplifications of spectral analysis at the studied irregularity levels.

In buildings with very low torsional irregularity, the seismic component in the transverse direction has minimal impact, and the analysis could be

performed considering only one of the components. However, this is not always the case for some buildings classified as regular according to NTE E.030.

When comparing the maximum amplifications from time-history analysis with those calculated using the combination of spectral responses, it is observed that the 100% rule yields amplification values that are closer to those obtained from time-history analysis in most cases.

The following graphs show that for regular structures, the $100\% - 30\%$ rule could be used, although it is not always conservative. For irregular structures, especially those with extreme irregularity, it would be necessary to perform the analysis with simultaneous action of 100% in both directions.
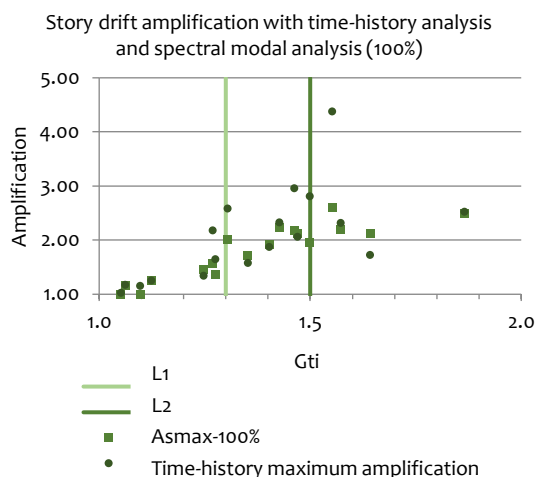
Fig. 14. Comparison of maximum amplifications between the results of spectral modal dynamic analysis using the 100% sum combination rule and time-history dynamic analysis
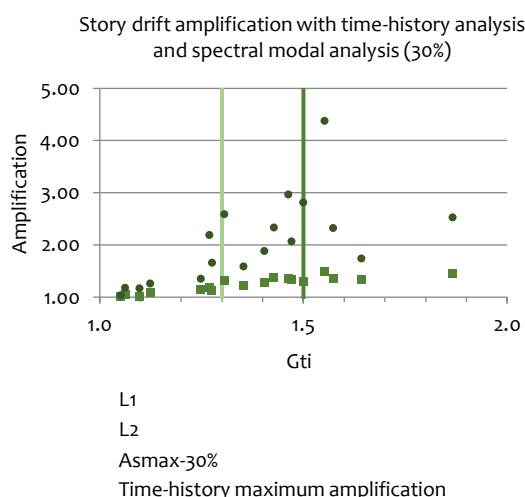

Fig. 12. Comparison of maximum amplifications between the results of spectral modal dynamic analysis using the 30% sum combination rule and time-history dynamic analysis.
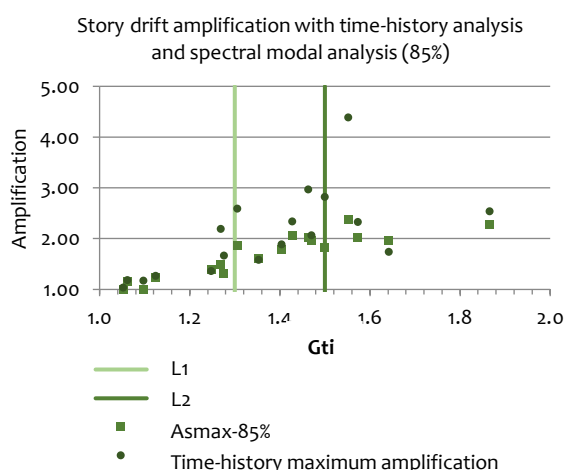
3.8. CQC3 Combination criterion

The CQC3 combination criterion involves calculating the maximum bidirectional response using the Complete Quadratic Combination (CQC). This response is determined by evaluating the response for an incidence angle known as the critical angle [17].

The maximum spectral amplification was calculated using the following formulas:

$$A_{SX} - CQC3 = \frac{\gamma_{X-CQC3}}{\gamma_{X,X}} \ldots\ldots\ldots\ldots(22)$$

$$A_{SY} - CQC3 = \frac{\gamma_{Y-CQC3}}{\gamma_{Y,Y}} \ldots\ldots\ldots\ldots(23)$$

$$A_{SMAX} - CQC3 = max(A_{SX} - CQC3, A_{SY} - CQC3) \ldots\ldots(24)$$

Where:

- γ_{X-CQC3}: Maximum inter-story drift in the X direction calculated from the unidirectional spectral modal analysis in X.
- γ_{Y-CQC3}: Maximum inter-story drift in the Y direction calculated from the unidirectional spectral modal analysis in Y.
- $A_{SMAX} - CQC3$: Maximum spectral amplification for the CQC3 combination.

The inter-story drift of the models were calculated using the CQC3 combination and compared with the maximum amplification from the time-history analyses. The results are presented in Fig. 15.

Fig. 13. Comparison of maximum amplifications between the results of spectral modal dynamic analysis using the 85% sum combination rule and time-history dynamic analysis.

Story drift amplification with time-history analysis
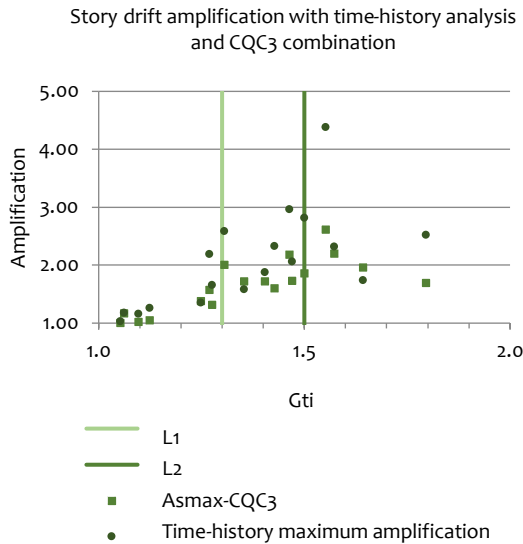and CQC3 combination

Fig. 15. Comparison of maximum amplifications between the
results of spectral modal dynamic analysis using the CQC3
combination rule and time-history dynamic analysis

From Fig. 15, comparing the maximum amplifications from time-history analysis with those calculated using the CQC3 combination, it is observed that the amplifications calculated with the time-history linear analysis are greater than those calculated with the CQC3 combination in most cases. It is also noted that, with respect to the degrees of torsional irregularity, the amplifications calculated using the CQC3 combination rule show an increasing trend for regular structures and those with moderate torsional irregularity. However, this trend starts to decrease for structures with extreme torsional irregularity.

CONCLUSIONS

- When considering the simultaneity of components in the simplified three-degree-of-freedom models, amplifications are observed to increase with the relative plan eccentricity and decrease with torsional rigidity.
- For the records used in this work, the simplified models analyzed in 3.4 show maximum amplifications on the order of 3 for models classified as regular according to the criteria of NTE E.030, around 4 for models with moderate torsional irregularity. In models with extreme torsional irregularity, amplifications greater than 14 are calculated for the theoretical case of lateral stiffness concentrated near the center of mass. In general, higher amplification values are observed. The amplification values presented in TABLE III for square-plan structures maintain the same order of magnitude for models with a side ratio of 1:2, as presented in TABLE IV.

- Comparing TABLE III and TABLE VI, it is concluded that the amplifications for the multi-story simplified models are lower than those for the single-story simplified models. For a torsional irregularity factor of $f = 0.1$, the amplifications are much smaller, decreasing from 14.26 to 2.85. Amplifications remain significant for torsional irregularity factors between 0.3 and 0.5.
- For structures analyzed in 3.6, the maximum simultaneity ratios do not show a clear trend with the degree of torsional irregularity. A ratio of up to 2.96 was obtained for the maximum inter-story drift in the one of the models, which has a torsional irregularity degree of 1.463. Structures with higher degrees of torsional irregularity have simultaneity ratios of up to 1.265. The maximum simultaneity ratios in existing real structures maintain the same order of magnitude as the amplifications calculated using simplified models. However, their variation is not as clearly correlated with the degree of torsional irregularity.
- It is concluded that the effect of simultaneity of seismic components in structures with torsional irregularity is significant and should be considered in the calculation of design responses.
- The summation combination rule with a 100% combination factor is the rule that best describes the potential amplification response of maximum design responses.
- There is no clear correlation between the amplification caused by the effect of simultaneous seismic components and the torsional irregularity index calculated in the same direction of analysis. However, a relationship was observed between the maximum amplification and the torsional irregularity index as defined in the E.030 standard, as shown in Figure 10.
- The amplifications calculated with the CQC3 combination rule show an increasing trend for regular structures and those with moderate torsional irregularity. However, this trend starts to decrease for structures with extreme torsional irregularity.

ACKNOWLEDGMENTS

REFERENCES

[1]SENCICO. (2020, July 29). EARTHQUAKE RESISTANT DESIGN, Technical standard for buildings E.030 [Online]. Available: https://www.gob.pe/institucion/sencico/informes-publicaciones/887225-normas-del-reglamento-nacional-de-edificaciones-rne.

[2] A. Fardis, Designers' Guide to Eurocode 8: Design of Structures for Earthquake Resistance – EN 1998-1 and EN 1998-5. London, UK: Thomas Telford, 2005. [Online]. Available: Designers' Guide to EN 1998-1 and 1998-5. Eurocode 8: Design Provisions for Earthquake Resistant Structures | Eurocodes: Building the future

[3] H. Tavera, Y. I. Bernal Esquia, C. Condori Quispe, M. Ordaz, A. Zevallos, and O. Ishizawa, Probabilistic Seismic Hazard Re-evaluation for Peru, Lima, Peru: Instituto Geofísico del Perú, 2014. [Online]. Available: https://repositorio.igp.gob.pe/items/8a770324-1619-4adc-b4a1-9cf94390ee91

[4] R. R. Youngs, S. J. Chiou, W. J. Silva, and J. R. Humphrey, "Strong ground motion attenuation relationships for subduction zone earthquakes", Seismological Research Letters, vol. 68, no. 1, pp. 58–73, 1997, doi: 10.1785/gssrl.68.1.58

[5] F. Sadigh, C. Y. Chang, J. Egan, F. Makdisi, and R. Youngs, "Attenuation relationships for shallow crustal earthquakes based on California strong motion data", Seismological Research Letters, vol. 68, no. 1, pp. 180–189, 1997, doi: 10.1785/gssrl.68.1.180

[6] Beyer K. y Bommer J., "Relationships between Median Values and between Aleatory Variabilities for Different Definitions of the Horizontal Component of Motion", Bulletin of the Seismological Society of America, vol.96, no. 4A, pp. 1512-1522, Aug. 2006, doi: 10.1785/0120050210

[7] Hisada T., Miyamura M., Kan S. y Hirao Y., "Studies on the Orthogonal Effects in Seismic Analyses", Proceedings of Ninth World Conference on Earthquake Engineering, vol. V pp 191-196, Tokyo- Kyoto, Japan, 1988. [Online]. Available: https://www.iitk.ac.in/nicee/wcee/ninth_conf_Japan/

[8] E. Moscoso, "Effect of Bidirectionality and Seismic Incidence Angle on the Response of Reinforced Concrete Structures," Master Thesis, Faculty of Civil Engineering, National University of Engineering, 2018. [Online]. Available: https://repositorio.uni.edu.pe/handle/20.500.14076/16380

[9] Fernandez V., Cominetti S. y Cruz E., "Considering the bi-directional effects and the seismic angle variations in building design", 12th World Conference on Earthquake Engineering; Auckland, New Zeland, 2000. [Online]. Available: https://www.nicee.org/wcee/index2.php

[10] ASCE. (2023). Minimum Design Loads for Buildings and Other Structures, ASCE/SEI 7-22 [Online]. Available: https://ascelibrary.org/doi/book/10.1061/9780784415788.

[11] R. Boroschek, P. Soto, and R. León, "Records of the Maule Earthquake Mw=8.8, February 27, 2010," Report RENADIC 10/05 Rev. 2, Oct. 2010. [Online]. Available: https://www.renadic.cl/red_archivos/RENAMAULE2010IR2.pdf

[12] R. Kosaka, E. Gonzales, H. Arias, A. Minaya, E. Farfán, y J. Ticona, "Evaluación de peligros de la Ciudad de Moquegua," Reporte, Convenio UNSA–INDECI, Arequipa, Sep. 2001. [En Linea]. Disponible https://sigrid.cenepred.gob.pe/sigridv3/documento/4401

[13] H. Tavera, I. Bernal, and H. Salas, " El sismo de Pisco del 15 de agosto, 2007 (7.9Mw), departamento de Ica – Perú (informe preliminar)", CNDG, IGP, Lima, Peru, 2007. [En Linea]. Disponible: https://repositorio.igp.gob.pe/items/9ebfc65c-a85c-400d-913e-12c570692a42

[14] P. Repetto, I. Arango, and B. Seed, "Influence of Characteristics on Building Damage During October 3, 1974 Lima Earthquake," Earthquake Engineering Research Center, Report No. UCB/EERC-80/41, 1980. [Online]. Available: https://nehrpsearch.nist.gov/article/PB81-161739/XAB

[15] SENCICO. (2020, November 20). Study on the Evaluation of the Simultaneity of Components in Structures with Torsional Irregularity [Online]. Available :

https://www.gob.pe/institucion/sencico/informes-publicaciones/1997409-estudio-de-evaluacion-de-la-simultaneidad-de-componentes-en-estructuras-con-irregularidad-torsional

[16] SENCICO. (2020, July 29). LOADS, Technical standard for buildings E.020 [Online]. Available : https://www.gob.pe/institucion/sencico/informes-publicaciones/887225-normas-del-reglamento-nacional-de-edificaciones-rne

[17] X. Gao, X. Zhou and L. Wang, "Multi-component seismic analysis for irregular structures", 13th World Conference on Earthquake Engineering, paper N°1156, Vancouver, B.C., Canada, Aug. 1-6,2004. [Online]. Available: https://www.iitk.ac.in/nicee/wcee/thirteenth_conf_Canada/